Journal of Applied Physics

RESEARCH ARTICLE | OCTOBER 09 2023

Stability of oscillator Ising machines: Not all solutions are created equal

Mohammad Khairul Bashar ; Zongli Lin ; Nikhil Shukla

J. Appl. Phys. 134, 144901 (2023)
https://doi.org/10.1063/5.0157107

Journal of Applied Physics ARTICLE pubs.aip.org/aip/jap

Stability of oscillator Ising machines: Not all solutions are created equal

Cite as: J. Appl. Phys. **134**, 144901 (2023); doi: 10.1063/5.0157107
Submitted: 5 May 2023 · Accepted: 20 September 2023 ·
Published Online: 9 October 2023

Mohammad Khairul Bashar, Zongli Lin, and Nikhil Shukla[a)]

AFFILIATIONS

Department of Electrical and Computer Engineering, University of Virginia, Charlottesville, Virginia 22904, USA

[a)]**Author to whom correspondence should be addressed:** ns6pf@virginia.edu

ABSTRACT

Nonlinear dynamical systems such as coupled oscillators are being actively investigated as Ising machines for solving computationally hard problems in combinatorial optimization. Prior works have established the equivalence between the global minima of the cost function describing the coupled oscillator system and the ground state of the Ising Hamiltonian. However, the properties of the oscillator Ising machine (OIM) from a nonlinear control viewpoint, such as the stability of the OIM solutions, remain unexplored. Therefore, in this work, using nonlinear control-theoretic analysis, we (i) identify the conditions required to ensure the functionality of the coupled oscillators as an Ising machine, (ii) show that all globally optimal phase configurations may not always be stable, resulting in some configurations being more favored over others and, thus, creating a biased OIM, and (iii) elucidate the impact of the stability of locally optimal phase configurations on the quality of the solution computed by the system. Our work, fostered through the unique convergence between nonlinear control theory and analog systems for computing, provides a new toolbox for the design and implementation of dynamical system-based computing platforms.

I. INTRODUCTION

Ising machines provide an elegant dynamical system platform for minimizing the Ising Hamiltonian $H = -\sum W_{ij}s_is_j$, where $s_i \in \{1,-1\}$ corresponds to the ith spin and W_{ij} is the interaction coefficient between nodes i and j; the Zeeman term has been neglected here. Minimizing H is a quintessential NP-hard combinatorial optimization problem (COP). Moreover, such systems are being actively investigated for solving many computationally challenging COPs, many of which can be directly mapped to the minimization of H.[1,2] An archetypal example of such a mapping is the MaxCut problem, which is defined as a graph cut that maximizes the number of cut edges (unweighted graph considered here). The relationship between H and the MaxCut (MC) can be defined as $H = \Sigma W - 2MC$, where ΣW is the sum of the weights of all the edges in the graph. Thus, the optimal MaxCut directly corresponds to the ground state (minimum H) of a topologically equivalent spin network with antiferromagnetic interactions, i.e., $W_{ij} = -1$. The promise of Ising machines is that allowing physics to do the computation can potentially provide a significant benefit in computational performance over digital algorithms.[3,4]

While the Ising model has been well known for many decades, recent interest in the field can be attributed to the development of quantum annealers (by companies such as D-wave[5]) with the objective of solving hard COPs while offering exponential speedup over digital algorithms. Since then, many technology platforms ranging from degenerate optical parametric oscillators,[6] spin waves,[7] bistable latches,[8] resonators,[9] memristors,[10] Kerr-nonlinear parametric oscillators,[11] spin torque nano-oscillators,[12] and electronic oscillators[13]—focus of the present work, have been used to design Ising machines. Coherent Ising machines, with sizes as large as 100 000 spins, have recently been realized using degenerate optical parametric oscillators.[14]

Coupled electronic oscillators are a promising candidate to realize Ising machines, commonly referred to as oscillator Ising machines (OIMs),[13] owing to their compactness and compatibility with integrated circuit (IC) technology. In groundbreaking work by Wang *et al.*,[13] the authors demonstrated that a global minimum of the cost function (referred to as the Lyapunov function by the authors) for a topographically equivalent coupled oscillator network under second harmonic injection can be equivalent to computing a global minimum of H. We have briefly summarized

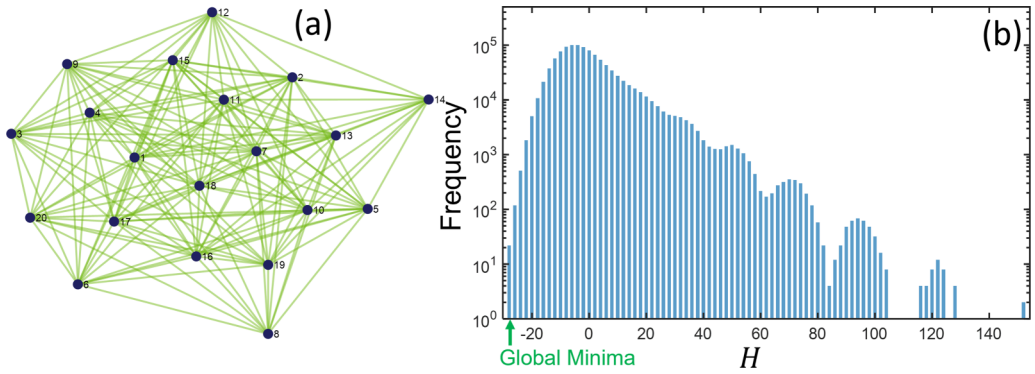

FIG. 1. (a) Illustrative randomly generated unweighted graph with 20 nodes and 152 edges. (b) Corresponding histogram of energy (H) for all (2^{20}) possible spin configurations.

this mapping in the Appendix for completeness. While the minimization of the cost function in OIMs[13] as well as their implementation[3,4,14–19] has been explored in prior work, the stability of the globally optimal and locally optimal spin (phase) configurations and the resulting impact on the OIM dynamics has been largely unexplored. The works by Erementchouk *et al.*[20] and Böhm *et al.*[21] are a few examples that aim to investigate the dynamics of the OIM, while a few more works have focused on analyzing the dynamical properties of the spiking neural network.[22–25] Consequently, understanding the properties of the OIM as a nonlinear dynamical system and elucidating their impact on the computational properties are the primary focus of this work.

II. RESULTS

The dynamics of the OIM are such that the oscillator phases settle to $\theta \in \{0, \pi\}$, which, subsequently, represent $s = \pm 1$ assignment to the nodes. The computational capability of this system arises from the fact that the resulting phase configuration of the oscillators will correspond to a ground state of H. The cost function $E(\theta(t))$ and the corresponding system dynamics are, respectively, presented as

$$E(\theta(t)) = -K \sum_{i,j=1,\, j\neq i}^{N} W_{ij}\cos\left(\theta_i - \theta_j\right) - K_s \sum_{i=1}^{N} \cos(2\theta_i(t)), \quad (1)$$

$$\frac{d\theta_i(t)}{dt} = -K \sum_{j=1,\ j\neq i}^{N} W_{ij}\sin\left(\theta_i - \theta_j\right) - K_s \sin(2\theta_i(t)), \quad (2)$$

where (W) represents the coupling matrix between nodes and K and K_s represent the strength of coupling among the oscillators and the strength of the second harmonic injection signal, respectively. For the MaxCut problem, the weight of an edge E_{ij} in the input graph is related to the coupling matrix by the relation $W_{ij} = -E_{ij}$. Using Eqs. (1) and (2), it can be shown that $\frac{dE(\theta)}{dt} = -2\sum_{i=1}^{N}\left(\frac{d\theta_i(t)}{dt}\right)^2 \leq 0$,[13,26] which consequently implies that the system will evolve toward the ground state, except when $\frac{dE(\theta)}{dt} = 0$ (i.e., $\frac{d\theta(t)}{dt} = 0$). A point in the phase space where $\frac{d\theta(t)}{dt} = 0$ defines a fixed point, and there are multiple such points in the phase space. In fact, every possible spin assignment and its equivalent in terms of the oscillator phases $\{\theta_1, \theta_2, \ldots, \theta_N\}$, where $\theta_i \in \{0, \pi\}$ can correspond to a fixed point. Consequently, the phase space contains 2^N fixed points in the system (for $\theta \in \{0, \pi\}$); 2^{N-1} points when symmetricity in the solutions is considered. The fixed points lying at the lowest energy, if stable, would correspond to an (globally) optimal solution to the Ising model, while stable fixed points that do not lie at the lowest energy would correspond to locally optimal (globally suboptimal) solutions. Furthermore, even for the same energy (including the ground state), some fixed points (i.e., spin configurations) may be stable, while others may not. This implies that the system may intrinsically favor certain Ising solutions over others, leading to a *biased OIM*. Consequently, engineering the system stability can have a significant impact on the computational characteristics and the performance of the system.

To elucidate our approach, we consider an illustrative randomly generated unweighted graph with 20 nodes and 152 edges as shown in Fig. 1(a). Figure 1(b) shows a histogram for the energy (quantified using H here) for all possible solutions. It can be observed in Fig. 1(b) that the graph has 22 spin configurations that yield the minimum energy ($H = -28$). However, as alluded to above, the system dynamics may not always be stable for all the 22 globally optimal configurations.

In order to investigate the stability of the globally and locally optimal phase configurations, we analyze the Lyapunov exponents ($\lambda_1, \lambda_2, \lambda_3, \ldots, \lambda_N$) for the system dynamics. Lyapunov exponents provide a powerful mathematical tool for analyzing the stability of non-linear dynamical systems.[27] Considering that dynamics are continuous-time, and the corresponding Jacobian matrix is symmetric,[28] the Lyapunov exponents are the same as the eigenvalues of the Jacobian matrix. For a phase configuration to be stable, all Lyapunov exponents should be negative. The Jacobian matrix (J) for the OIM (assuming symmetric unweighted edges, i.e., $W_{ij} = W_{ji}$) can be defined as

$$J = \begin{bmatrix} E(1,1) & -KW_{12}\cos(\theta_1-\theta_2) & -KW_{13}\cos(\theta_1-\theta_3) & \cdots & -KW_{1N}\cos(\theta_1-\theta_N) \\ -KW_{12}\cos(\theta_1-\theta_2) & E(2,2) & -KW_{23}\cos(\theta_2-\theta_3) & \cdots & \\ -KW_{13}\cos(\theta_1-\theta_3) & -KW_{23}\cos(\theta_2-\theta_3) & E(3,3) & & \\ \vdots & \vdots & \vdots & \cdots & \vdots \\ -KW_{1N}\cos(\theta_1-\theta_N) & & \cdots & & E(N,N) \end{bmatrix}, \quad (3)$$

where $E(i,i) = -K\sum_{j=1,j\neq i}^{N} W_{ij}\cos(\theta_i-\theta_j) - 2K_s\cos(2\theta_i)$. The eigenvalues of J for a given point in the phase space where $\frac{d\theta(t)}{dt} = 0$ yield the Lyapunov exponents at that point. Since *all* the Lyapunov exponents need to be negative in order for an energy minimum to be stable, we focus on the largest Lyapunov exponent (referred to here as λ_L) since all other exponents will be smaller than λ_L.

Figure 2(a) shows the evolution of the *largest* Lyapunov exponent (λ_L) as a function of K_s ($K = 1$) for the representative graph shown in Fig. 1(a). All the 2^{20} possible phase configurations are considered. The evolution of λ_L for only the globally optimal solutions is emphasized in Fig. 2(b). It can be observed that the stability of a spin configuration is significantly impacted by the strength K_s (relative to K) of the second harmonic injection signal. In fact, if K_s is small enough (<0.5 for the graph considered here), then the ground states, i.e., globally optimal configurations, themselves can become unstable. In such a scenario, the system will cease to behave as an Ising machine—the ground state energy of the system will then correspond to an oscillator phase configuration where some or all oscillator phases do not settle to 0 or π.

Next, for different K_s ($K = 1$), we analyze the distribution of λ_L for all phase configurations lying at a given energy (H). Figures 3(a)–3(c) show the maximum and the minimum value of λ_L for phase configurations corresponding to a given H, computed for three different values of K_s (0.1, 0.8, and 1.5), respectively. In Fig. 3(a), it can be observed that since λ_L for all spin configurations (including the globally optimal solutions lying at $H = -28$) are greater than zero, the ground state of the oscillator platform will not be achieved for $\theta \in \{0, \pi\}$. Consequently, it is expected that the oscillator platform will cease to function as an Ising machine. When $K_s = 0.8$ [Fig. 3(b)], it can be observed that the maximum and the minimum values of λ_L for the globally optimal solutions straddle zero; i.e., λ_L for some solutions is less than zero, whereas it is greater than zero for others. This implies that only a fraction of the globally optimal spin configurations is stable, and consequently, the system dynamics will preferentially converge to the stable (globally optimal) solutions. This creates a biased OIM that favors the stable states over the unstable ones. Additionally, it is also noteworthy to point out that some of the fixed points corresponding to locally optimal (but globally sub-optimal) solutions lying at low energies ($H = -24, -26$) are also stabilized. This indicates that the system may potentially get trapped in one of these states, leading to sub-optimal solutions. However, the value of K_s is such that the solutions lying at higher energies ($H > -24$) are destabilized, preventing the system from getting trapped in those states. Finally, when the strength of the second harmonic injection is increased further to $K_s = 1.5$ [Fig. 3(c)], it can be observed that all the globally optimal solutions are stabilized. Additionally, increasing the strength of the second harmonic injection also increases the number and energy of the locally optimal (globally sub-optimal) solutions where the system dynamics can be stabilized. Consequently, this should increase the probability of the system getting trapped at a local minimum. Here, we only consider the

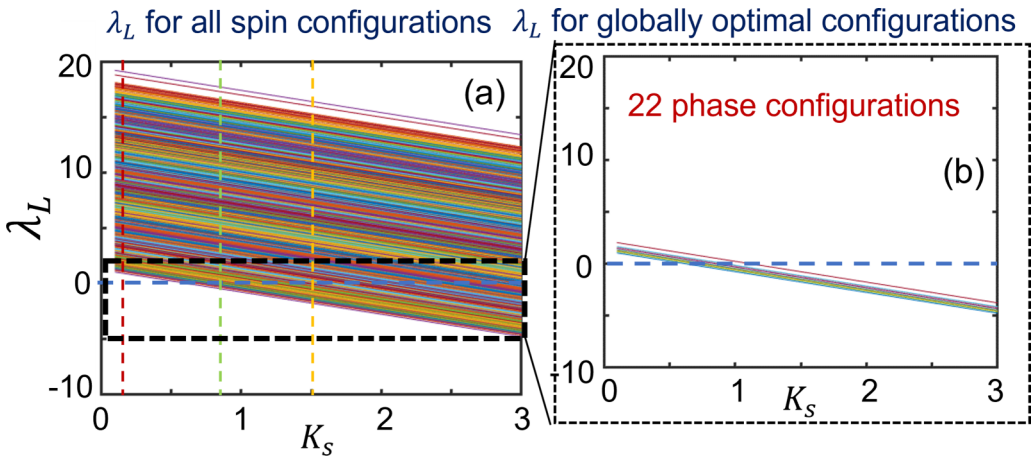

FIG. 2. (a) Evolution of the largest Lyapunov exponent (λ_L) as a function of K_s for all spin configurations; (b) evolution of λ_L as a function of K_s for the subset of globally optimal phase configurations. Note that $\lambda_L > 0$ implies that the particular solution is unstable.

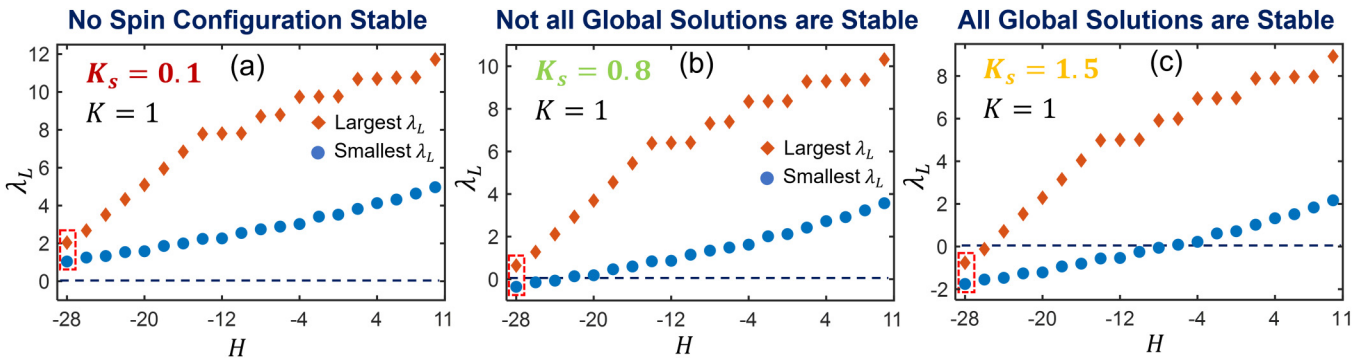

FIG. 3. Minimum (blue) and maximum (orange) λ_L for phase configurations lying at a particular energy (H). Three values of K_s are considered—(a) $K_s = 0.1$ since all spin configurations (including the globally optimal solutions) are unstable, it implies that the oscillator platform will cease to behave as an Ising machine. (b) $K_s = 0.8$: some globally optimal solutions are stable, while others are unstable. Additionally, a few locally optimal low energy solutions are also stabilized; (c) $K_s = 1.5$: all globally optimal solutions are stable. The red box indicates the globally optimal solutions.

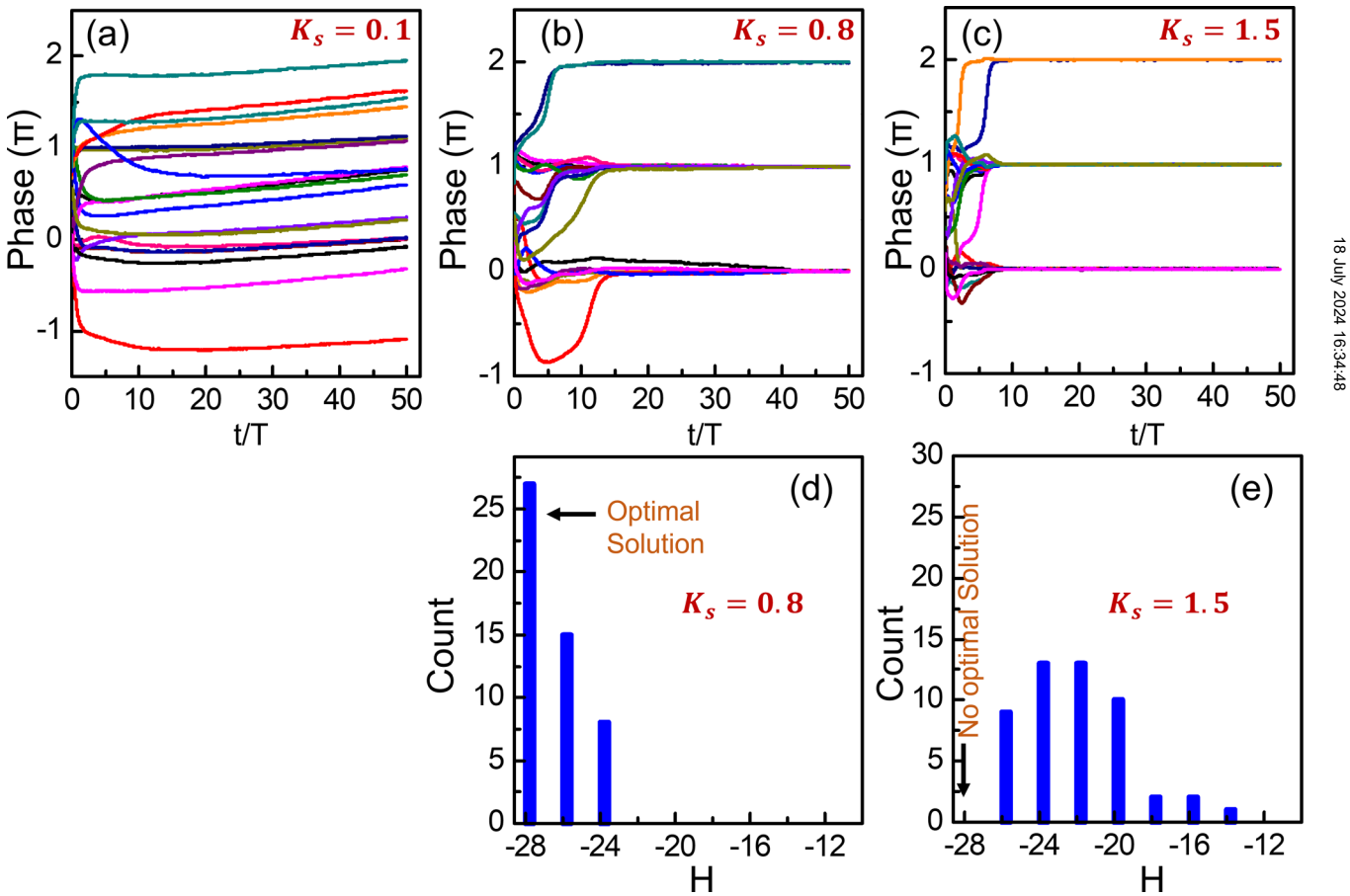

FIG. 4. Temporal evolution of the oscillator phases for (a) $K_s = 0.1$, (b) $K_s = 0.8$, (c) $K_s = 1.5$ ($K = 1$). The oscillator network is topologically equivalent to the graph considered in Fig. 1(a). When $K_s = 0.1$, the phases do not converge to $\{0, \pi\}$, and thus, the system does not behave as an Ising machine. Measured H for (d) $K_s = 0.8$ and (e) $K_s = 1.5$ over 50 trials. Since a smaller number of locally optimal solutions are stabilized at $K_s = 0.8$ compared to $K_s = 1.5$, the system yields better solution quality. No solution is obtained for $K_s = 0.1$.

fixed points associated with Ising solutions ($\theta \in \{0, \pi\}$). There may be other fixed points in the phase space corresponding to configurations where $\theta \notin \{0, \pi\}$. We also note that for the OIM dynamics, the stability of the fixed points can also be alternatively analyzed by using the second-order partial derivative test.

We verify the system behavior predicted above using simulations shown in Fig. 4. We consider an oscillator network that is equivalent to the graph considered in Fig. 1(a) and, subsequently, evaluate the dynamics for different second harmonic injection strengths. We simulate system dynamics (2) using a MATLAB's® SDE (stochastic differential equation) solver, where we consider a time and phase independent noise amplitude of $K_n = 0.005$. When $K_s = 0.1$, the oscillator phases, as expected, do not converge to $\{0, \pi\}$ and the oscillator platform does not behave as an Ising machine. For larger injection strengths ($K_s = 0.8,\ 1.5$), it can be observed that the oscillator phases are binarized to $\{0, \pi\}$, validating the system's ability to function as an Ising machine.

Figures 4(d) and 4(e) show a histogram of the computed H for $K_s = 0.8$ and $K_s = 1.5$, respectively, over 50 trials with randomly generated initial conditions. The spin assignments and the solutions are not computed for $K_s = 0.1$ since the system does not behave as an Ising machine. Since $K_s = 0.8$ only stabilizes some globally optimal solutions and some phase configurations that lie at low energy ($H = -26, -24$), it can be observed that the system dynamics always converge to one of these states. In contrast, increasing the second harmonic injection strength to $K_s = 1.5$ stabilizes all the 22 global solutions as well as many other phase configurations that lie at higher energies [Fig. 3(c)]. Consequently, it can be observed in Fig. 4(e) that the system dynamics exhibit a higher probability of getting trapped at a local minimum (suboptimal spin configuration). In fact, over 50 trials, the system never converges to a globally optimal solution ($H = -28$). This indicates that the ability to engineer the stability of the local minima can significantly impact the computational performance of the OIM.

III. CONCLUSION

OIMs are being actively investigated for solving computationally hard problems in combinatorial optimization. While such problems find extensive practical applications in fields ranging from resource optimization to financial arbitrage, many of these problems are still considered intractable to solve efficiently using digital algorithms. Hence, Ising machines have the potential of creating a transformative impact. While there have been many demonstrations of Ising machines using a plethora of hardware technologies, a principled approach to designing such systems remains less explored.

In this work, we have uniquely examined the OIM design from a control theoretic standpoint. By calculating the Lyapunov exponents for various spin configurations, we analyze the stability of the globally and locally optimal solutions. We show that not all globally optimal phase configurations may always be stable, in which case the system behaves as a biased OIM. Furthermore, our analysis also provides insights into the stability of the locally optimal phase configurations, which can significantly impact the probability of the system dynamics getting trapped at a local minimum. Subsequently, this impacts the quality of the solution computed by the system. Thus, this work presents a novel paradigm rooted in nonlinear control theory for analyzing dynamical system-based computing platforms such as OIMs and creates a new toolkit for the design and implementation of such systems.

ACKNOWLEDGMENTS

This work was supported by NSF Grant No. 2132918.

AUTHOR DECLARATIONS

Conflict of Interest

The authors declare no competing interests.

Author Contributions

Mohammad Khairul Bashar: Formal analysis (equal); Software (lead); Writing – original draft (supporting). **Zongli Lin:** Validation (lead); Writing – review & editing (lead). **Nikhil Shukla:** Conceptualization (lead); Formal analysis (equal); Project administration (lead); Software (supporting); Supervision (lead); Writing – original draft (lead).

DATA AVAILABILITY

The data that support the findings of this study are available from the corresponding author upon reasonable request.

APPENDIX: THEORETICAL FRAMEWORK FOR OSCILLATOR ISING MACHINE

The theoretical framework showing how coupled oscillator under second harmonic injection works as an oscillator Ising machine is shown by Wang *et al.*[13] For completeness, we briefly summarize this here.

The generalized Adler's equation representing the phase dynamics of a perturbed (or a coupled) oscillator can be shown as

$$\frac{\mathrm{d}}{\mathrm{d}t}(\theta\ (t)) = \omega_0 - \omega_b + \omega_0\ C(\theta(t) - \theta_b(t)). \tag{A1}$$

Here, $\theta(t)$ and $\theta_b(t)$ are oscillator's phase and perturbation's phase, respectively; ω_0 and ω_b are the oscillator's frequency and the perturbation's frequency, respectively; $C(.)$ is the perturbation projection vector (PPV) of the oscillator that quantifies the oscillator's phase response when a perturbation acts on it. Using Eq. (A1), the phase dynamics of the ith oscillator in an N-coupled oscillator system can be represented as

$$\frac{d}{dt}(\theta_i\ (t)) = \omega_i - \omega_n + \omega_i \sum_{j=1, j\neq i}^{N} C_{ij}\big(\theta_i(t) - \theta_j(t)\big), \tag{A2}$$

where ω_n is the natural frequency of the oscillators and ω_i is the frequency of the ith oscillator. If the oscillators are sinusoidal and oscillating with their natural frequency ω_n, under the presence of a

second harmonic injection, Eq. (A2) can be written as

$$\frac{d\theta_i(t)}{dt} = -K \sum_{j=1,\ j\neq i}^{N} W_{ij}\sin\left(\theta_i - \theta_j\right) - K_s\sin(2\theta_i(t)). \quad \text{(A3)}$$

Here, W_{ij} is the coupling weight between oscillators i and j.

For the dynamics shown in Eq. (A3), a cost function E can be defined such that $-\nabla E = \dot{\theta}$. It is shown as

$$E(\theta(t)) = -K \sum_{i,j=1,\ j\neq i}^{N} W_{ij}\cos\left(\theta_i - \theta_j\right) - K_s \sum_{i=1}^{N}\cos(2\theta_i(t)). \quad \text{(A4)}$$

Furthermore,

$$\begin{aligned}\frac{\partial E(\theta(t))}{\partial \theta_i} &= K \sum_{l=1,\ l\neq i}^{N} W_{il}\sin(\theta_i - \theta_l) + K \sum_{m=1,\ m\neq i}^{N} \sin(\theta_m - \theta_i) \\ &\quad + 2K_s\sin(2\theta_i(t)), \\ &= -2\left[-K \sum_{j=1,\ j\neq i}^{N} W_{ij}\sin(\theta_i - \theta_j) - K_s\sin(2\theta_i(t))\right] \\ &= -2\frac{d\theta_i(t)}{dt}.\end{aligned} \quad \text{(A5)}$$

Hence,

$$\frac{dE(\theta(t))}{dt} = \sum_{i=1}^{N} \frac{\partial E(\theta(t))}{\partial \theta_i}\frac{d\theta_i}{dt} = -2\sum_{i=1}^{N}\left(\frac{d\theta_i}{dt}\right)^2 \leq 0. \quad \text{(A6)}$$

Equation (A6) shows that $\frac{dE(\theta(t))}{dt} \leq 0$; i.e., $E(\theta(t))$ does not increase with time. Furthermore, at the specific phase points $\theta \in \{0, \pi\}$, which map to the spin states $s \in \{1, -1\}$ in the Ising Hamiltonian, and $K = 1/2$, Eq. (A4) is equivalent to the Ising Hamiltonian H with a constant offset,[26]

$$E(\theta(t)) = -\sum_{i,j,i<j}^{N} W_{ij}\cos(\theta_i - \theta_j) - NK_s. \quad \text{(A7)}$$

The coupling weights W_{ij} represent the weight of the edges E_{ij} of the graph to be solved. For the MaxCut problem, the coupling weights are calculated using the relationship $W_{ij} = -E_{ij}$; when no edge is present, $E_{ij} = 0$. This relationship arises from the fundamental mapping between solving the MaxCut problem and the minimization of the Ising Hamiltonian.[1]

REFERENCES

[1]A. Lucas, Front. Phys. **2**, 5 (2014).
[2]G. Csaba and W. Porod, Appl. Phys. Rev. **7**, 011302 (2020).
[3]A. Mallick, M. K. Bashar, D. S. Truesdell, B. H. Calhoun, and N. Shukla, in *2021 IEEE International Electron Devices Meeting (IEDM)* (IEEE, 2021), pp. 40.2.1–40.2.4.
[4]J. Chou, S. Bramhavar, S. Ghosh, and W. Herzog, Sci. Rep. **9**, 14786 (2019).
[5]D-Wave Advantage, retrieved on August 5, 2023. At: https://www.dwavesys.com/solutions-and-products/systems/.
[6]T. Inagaki, Y. Haribara, K. Igarashi, T. Sonobe, S. Tamate, T. Honjo, A. Marandi, P. L. McMahon, T. Umeki, K. Enbutsu, O. Tadanaga, H. Takenouchi, K. Aihara, K.-I. Kawarabayashi, K. Inoue, S. Utsunomiya, and H. Takesue, Science **354**, 603–606 (2016).
[7]A. Litvinenko, R. Khymyn, V. H. González, R. Ovcharov, A. A. Awad, V. Tyberkevych, A. Slavin, and J. Åkerman, Commun. Phys. **6**, 227 (2023).
[8]A. Mallick, Z. Zhao, M. K. Bashar, S. Alam, M. M. Islam, Y. Xiao, Y. Xu, A. Aziz, V. Narayanan, K. Ni, and N. Shukla, Sci. Rep. **13**, 1515 (2023).
[9]L. Q. English, A. V. Zampetaki, K. P. Kalinin, N. G. Berloff, and P. G. Kevrekidis, Commun. Phys. **5**, 333 (2022).
[10]F. Cai, S. Kumar, T. Van Vaerenbergh, X. Sheng, R. Liu, C. Li, Z. Liu, M. Foltin, S. Yu, Q. Xia, J. J. Yang, R. Beausoleil, W. D. Lu, and J. P. Strachan, Nat. Electron. **3**, 409–418 (2020).
[11]T. Kanao and H. Goto, npj Quantum Inf. **7**, 18 (2021).
[12]D. I. Albertsson, M. Zahedinejad, A. Houshang, R. Khymyn, J. Åkerman, and A. Rusu, Appl. Phys. Lett. **118**, 112404 (2021).
[13]T. Wang, L. Wu, P. Nobel, and J. Roychowdhury, Nat. Comput. **20**, 287–306 (2021).
[14]T. Honjo, T. Sonobe, K. Inaba, T. Inagaki, T. Ikuta, Y. Yamada, T. Kazama, K. Enbutsu, T. Umeki, R. Kasahara, K. I. Kawarabayashi, and H. Takesue, Sci. Adv. **7**, eabh0952 (2021).
[15]M. K. Bashar, A. Mallick, D. S. Truesdell, B. H. Calhoun, S. Joshi, and N. Shukla, IEEE J. Explor. Solid-State Comput. Devices Circuits **6**, 116–121 (2020).
[16]S. Dutta, A. Khanna, A. S. Assoa, H. Paik, D. G. Schlom, Z. Toroczkai, A. Raychowdhury, and S. Datta, Nat. Electron. **4**, 502–512 (2021).
[17]N. Mohseni, P. L. McMahon, and T. Byrnes, Nat. Rev. Phys. **4**, 363–379 (2022).
[18]G. V. Joseph, "Ising machines and spiking neural networks: Non von-Neumann computing using networks of coupled oscillators" Ph.D. thesis (University College Dublin, School of Mechanical and Materials Engineering, 2021).
[19]A. Houshang, M. Zahedinejad, S. Muralidhar, J. Chęciński, R. Khymyn, M. Rajabali, H. Fulara, A. A. Awad, M. Dvornik, and J. Åkerman, Phys. Rev. Applied **17**, 014003 (2022).
[20]M. Erementchouk, A. Shukla, and P. Mazumder, Phys. D: Nonlinear Phenom. **437**, 133334 (2022).
[21]F. Böhm, T. V. Vaerenbergh, G. Verschaffelt, and G. Van der Sande, Commun. Phys. **4**, 149 (2021).
[22]E. P. Frady and F. T. Sommer, Proc. Natl. Acad. Sci. U. S. A. **116**, 18050–18059 (2019).
[23]Q. L. Gu, Z. K. Tian, G. Kovačič, D. Zhou, and D. Cai, Front. Comput. Neurosci. **12**, 47 (2018).
[24]S. Nobukawa, H. Nishimura, T. Yamanishi, and J.-Q. Liu, PLoS One **10**, e0138919 (2015).
[25]S. Nobukawa, H. Nishimura, and T. Yamanishi, Sci. Rep. **8**, 379 (2018).
[26]A. Mallick, M. K. Bashar, Z. Lin, and N. Shukla, Phys. Rev. Appl. **17**, 064064 (2022).
[27]B. Sándor, B. Schneider, Z. I. Lázár, and M. Ercsey-Ravasz, Entropy **23**, 103 (2021).
[28]D. K. Arrowsmith and C. M. Place, *Dynamical Systems: Differential Equations, Maps, and Chaotic Behaviour* (Chapman & Hall, 1992).